Label-Free Molecular Interaction Determinations with Nanoscale Interferometry

Dmitry A. Markov,[†] Kelly Swinney,[‡] and Darryl J. Bornhop*,[†]

Contribution from the Department of Chemistry, Vanderbilt University, VU Station B 351822, Nashville, Tennessee 37235-1822, and Johnson & Johnson Pharmaceutical Research and Development, 1000 Route 202, Box 300, Raritan, New Jersey 08869

Received April 15, 2004; E-mail: darryl.bornhop@vanderbilt.edu

Abstract: Quantification of protein−protein and ligand−substrate interactions is central to understanding basic cellular function and for evaluating therapeutics. To mimic biological conditions, such studies are best executed *without* modifying the proteins or ligands (i.e., label-free). While tools for label-free assays exist, they have limitations making them difficult to fully integrate into microfluidic devices. Furthermore, it has been problematic to reduce detection volumes for *on-channel* universal analyte quantification without compromising sensitivity, as needed in label-free methods. Here we show how backscattering interferometry in rectangular channels (BIRC) facilitates label-free studies within picoliter volumes. The simple and unique optical train was based on rectangular microfluidic channels molded in poly(dimethylsiloxane) and low-power coherent radiation. Quantification of irreversible streptavidin−biotin binding and *reversible* protein A−human IgG F_c molecular interactions in a 225 pL detection volume was carried out label-free and noninvasively. Detection limits of 47×10^{-15} mol of biotin reacted with surface-immobilized streptavidin were achieved. In the case of reversible interactions of protein A and the F_c fragment of human IgG, detection limits were determined to be 2×10^{-15} mol of IgG F_c. These experiments demonstrate for the first time that (1) high-sensitivity universal solute quantification is possible using interferometry performed within micrometer-sized channels formed in inexpensive PDMS chips, (2) label-free reversible molecular interaction can be studied with femtomoles of solute, and (3) BIRC has the potential to quantify binding affinities in a high-throughput format.

Introduction

Many challenges exist in the proteomics field.[1−6] If human health and therapeutic potential are to become true beneficiaries in this discipline, vast numbers of proteins need to be identified and their interactions and functions fully understood. To be fully effective, proteomic determinations should be performed minus any chemical labeling or derivatization. Label-free assays allow the study of proteins and their ligands in the native state to retain more biological purity and more closely mimic biological activity. Additionally, pharmaceutical potential can be more fully interrogated. It is also desirable to perform label-free determinations in a high-throughput format,[1−8] particularly for probing therapeutic potential. Often, proteins or ligands of interest are in short supply, are contained in small volumes, or need to be screened against numerous substrates. These constraints challenge conventional sample manipulation and detection schemes, yet microfabricated bioanalytical devices represent ideal platforms for such analyses. While several label-free analysis techniques have been demonstrated,[7,9−11] one that is fully compatible with microfluidics, provides universal response, is noninvasive, highly sensitive, and cost-effective, and has the potential to be quantitative has yet to be demonstrated.

A widely accepted technique, surface plasmon resonance (SPR), can be used to perform label-free molecular interaction assays.[9,10,12−14] SPR is based on measuring the change in local refractive index (RI) near the gold surface when the immobilized target reacts with the ligand or analyte molecule. Several approaches have been developed to improve detection limits, including the addition of metallic or colloidal particles to the analyte solution.[15−17] However, these techniques remain unde-

---

[†] Vanderbilt University.

[‡] Johnson & Johnson Pharmaceutical Research and Development.

(1) Fields, S. *Science* **2001**, *291*, 1221−1222.
(2) Rothmund, M.; Schutz, A.; Brecht, A.; Gauglitz, G.; Berthel, G.; Grafe, D. *Fresenius' J. Anal. Chem.* **1997**, *359*, 15−22.
(3) Hu, S.; Dovichi, N. J. *Anal. Chem.* **2002**, *74*, 2833−2850.
(4) Lion, N.; Rohner, T. C.; Dayon, L.; Arnaud, I. L.; Damoc, E.; Youhnovski, N.; Wu, Z. Y.; Roussel, C.; Josserand, J.; Jensen, H.; Rossier, J. S.; Przybylski, M.; Girault, H. H. *Electrophoresis* **2003**, *24*, 3533−3562.
(5) Marko-Varga, G.; Nilsson, J.; Laurell, T. *Electrophoresis* **2003**, *24*, 3521−3532.
(6) Mocellin, S.; Rossi, C. R.; Traldi, P.; Nitti, D.; Lise, M. *Trends Mol. Med.* **2004**, *10*, 24−32.
(7) Dancil, K.-P. S.; Greiner, D. P.; Sailor, M. J. *J. Am. Chem. Soc.* **1999**, *121*, 7925−7930.
(8) Broach, J. R.; Thorner, J. *Nature* **1996**, *384*, 14−16.

(9) Jordan, C. E.; Frutos, A. G.; Thiel, A. J.; Corn, R. M. *Anal. Chem.* **1997**, *69*, 4939−4947.
(10) Nelson, B. P.; Grimsrud, T. E.; Liles, M. R.; Goodman, R. M.; Corn, R. M. *Anal. Chem.* **2001**, *73*, 1−7.
(11) Lin, V. S. Y.; Motesharei, K.; Dancil, K. P. S.; Sailor, M. J.; Ghadiri, M. R. *Science* **1997**, *278*, 840−843.
(12) Boussaad, S.; Pean, J.; Tao, N. J. *Anal. Chem.* **2000**, *72*, 222−226.
(13) Sota, H.; Hasegawa, Y.; Iwakura, M. *Anal. Chem.* **1998**, *70*, 2019−2024.
(14) Lahiri, J.; Isaacs, L.; Tien, J.; Whitesides, G. M. *Anal. Chem.* **1999**, *71*, 777−790.
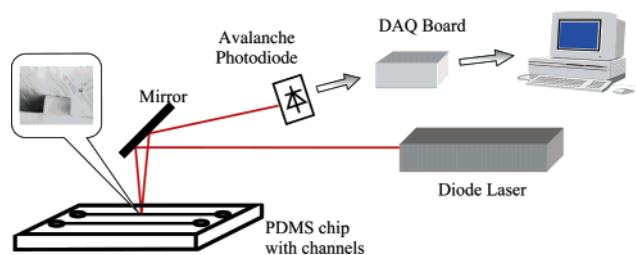(15) Lyon, L. A.; Musick, M. D.; Natan, M. J. *Anal. Chem.* **1998**, *70*, 5177−5183.

Figure 1. Block diagram of the BIRC setup. The highlighted magnified area of the PDMS chip at the left shows a cross-section of the typical rectangular channel molded in PDMS.

sirable due to the invasive nature of the approach and the difficulty in adapting them for high-throughput analysis. At the expense of increasing the instrumental complexity, imaging SPR has allowed an array format to be implemented, significantly improving the utility of the technique.[18−20] Even though SPR is a powerful technique for label-free molecular interaction determinations, it remains limited by the requirement of gold-plated substrates and high-quality optical prisms, somewhat complicated flow-cell designs for sample delivery, solute detection only in close proximity (within nanometers) of the gold surface,[9,10,12−14] and an inherent incompatibility with microfluidic systems.

Alternatively, Sailor and co-workers have shown that a porous silicon detector based on a Fabry−Perot interferometer can be used to study reversible protein−protein binding interactions and DNA hybridization reactions.[7,11,21] By illuminating the sensor from the top, Sailor et al.[7,11,21] were able to overcome one major shortcoming of SPR, a limited penetration depth, and detect changes in the mass of immobilized protein or DNA far above the sensor's surface.[7,11] Although the porous silicon sensor showed good performance and reasonable detection limits, diffusion-limited reaction times (∼100 min for IgG) and long sensor surface preparation times (7 h) preclude the use of this technique for flowing streams and restrict its use to static measurements where response time is not an issue.[7] Thus, integration of the porous Si detection system into a microfluidic network appears to be problematic.

Among the most promising techniques for nanoscale universal solute quantification with microfluidic systems is backscattering interferometry.[22−26] The on-chip interferometric backscatter detector employs a simple optical train comprised of a coherent light source (commonly a low-power He−Ne or red diode laser), a microfluidic channel formed in glass, fused silica, or plastic, and a phototransducer (Figure 1). The interaction of the laser beam with the fluid-filled channel results in a high-contrast interference pattern as shown in Figure 2. The intensity profile

of this fringe pattern changes in a predictable manner[22,24,25,27] with optical path length changes. Analysis of fringe positional changes, performed by a phototransducer located in the direct backscatter direction,[25] has facilitated the measurement of RI changes with resolution on the order of 10^{-6} within a 188 pL volume. Earlier configurations of the on-chip interferometric backscatter detector allowed label-free protein quantification in on-chip CE,[26,28] noninvasive nanoliter thermometry,[29] and highly accurate nanoscale noninvasive flow sensing.[30]

Presented in this paper is a new approach for noninvasive label-free molecular interaction determinations based on back-scattering interferometry in rectangular channels (BIRC) that is fully compatible with microfluidics, making it one of the few methodologies compatible with high-throughput screening. The technique uses a unique and surprisingly simple optical train, allowing undemanding fabrication and inexpensive chip manu-facturing processes to be employed. First, the well-characterized, high-binding-affinity, biotin and streptavidin pair was studied, showing that BIRC can quantify irreversible molecular binding events. The detection limit for biotin was found to be 47 fmol. Second, reversible protein−protein interactions were studied using the protein A and IgG couple. Repetitive protein binding events could be monitored without the need for fluorescent or radioactive labels in picoliter volumes. Detection limits indicate that label-free IgG binding can be quantified at the level of 2 fmol.

These microfluidic-based molecular interaction determinations were made possible using a substantially refined version of on-chip interferometric backscatter detection (OCIBD), backscat-tering interferometry in rectulangular channels. Previously, etched fused silica chips requiring nontrivial manufacturing with *curved* surfaces were used. The channels in these chips are conducive to multipass sensitivity enhancements because (1) they are inherently smooth, leading to good reflectivity, and (2) the curved optical surface formed during isotropic etch acts as a lens, refracting or focusing the incoming beam.[22−25,27] The new approach to on-chip interferometry described here employs *rectangular* channels molded within poly(dimethylsiloxane) (PDMS) chips. These channels are not coated to enhance surface reflectivity. It is not obvious or intuitive nor did simple ray tracing indicate that it would be possible to perform *high-sensitivity* interferometry with molded−stamped rectangular PDMS channels. Interestingly, the fringe pattern intensity distribution is different for BIRC than for OCIBD with entire regions of fringes missing. Even so, BIRC responds linearly with solute concentration, and allows for the quantification of RI changes on the order of 8×10^{-6} in a detection volume of 225 pL. BIRC is a significant improvement over our previously reported OCIBD system that facilitates label-free molecular interaction assays.

Experimental Section

BIRC Setup. The block diagram of the experimental setup is shown in Figure 2. A PDMS microfluidic chip was securely mounted onto an insulated massive black anodized aluminum block, which provided

(16) Haes, A. J.; Van Duyne, R. P. *J. Am. Chem. Soc.* **2002**, *124*, 10596−10604.
(17) Sun, Y. G.; Xia, Y. N. *Anal. Chem.* **2002**, *74*, 5297−5305.
(18) Wegner, G. J.; Lee, N. J.; Marriott, G.; Corn, R. M. *Anal. Chem.* **2003**, *75*, 4740−4746.
(19) Smith, E. A.; Thomas, W. D.; Kiessling, L. L.; Corn, R. M. *J. Am. Chem. Soc.* **2003**, *125*, 6140−6148.
(20) Lee, H. J.; Goodrich, T. T.; Corn, R. M. *Anal. Chem.* **2001**, *73*, 5525−5531.
(21) Doan, V. V.; Sailor, M. J. *Science* **1992**, *256*, 1791−1792.
(22) Swinney, K.; Markov, D.; Bornhop, D. J. *Rev. Sci. Instrum.* **2000**, *71*, 2684−2692.
(23) Bornhop, D. J. *Appl. Opt.* **1995**, *34*, 3234−3239.
(24) Swinney, K.; Markov, D.; Hankins, J.; Bornhop, D. J. *Anal. Chim. Acta* **1999**, *400*, 265−280.
(25) Swinney, K.; Markov, D.; Bornhop, D. J. *Anal. Chem.* **2000**, *72*, 2690−2695.
(26) Swinney, K.; Bornhop, D. J. *Analyst* **2000**, *125*, 1713−1717.

(27) Sorensen, H. S.; Pranov, H.; Larsen, N. B.; Bornhop, D. J.; Andersen, P. E. *Anal. Chem.* **2003**, *75*, 1946−1953.
(28) Wang, Z. L.; Swinney, K.; Bornhop, D. J. *Electrophoresis* **2003**, *24*, 865−873.
(29) Swinney, K.; Bornhop, D. J. *Electrophoresis* **2001**, *22*, 2032−2036.
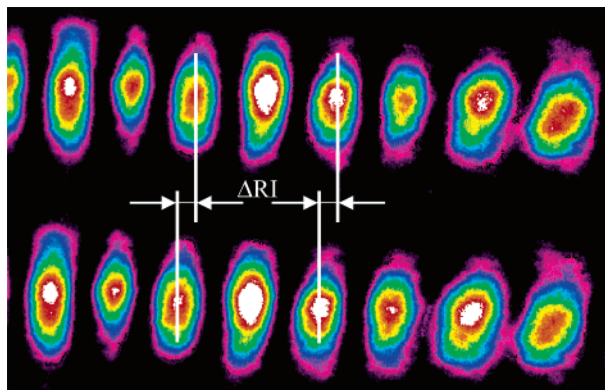(30) Markov, D. A.; Bornhop, D. J. *Fresenius' J. Anal. Chem.* **2001**, *371*, 234−237.

Figure 2. False color reconstruction of a typical backscattered interference pattern produced by BIRC with rectangular channels molded in PDMS. The change in fringe position corresponds to the refractive index change of 6×10^{-4} RIU.

passive thermal stabilization for the chip. A mirror, located 5 cm above the chip surface and mounted at an approximately 45° angle with respect to the incoming beam, served to divert the incoming laser beam from the semiconductor laser (μ-Laser Corp.) onto the sample channel and to redirect the resulting backscattered interference fringe pattern onto a photodetector. The laser wavelength was 633 nm, and the beam diameter was 75 μm. The phototransducer consisted of a small-area avalanche photodiode (300 μm diameter) which was reverse-biased with 212 V to operate near breakdown. The photodetector output was digitized using a PPIO-AI08 data acquisition board (Cyber Research, Inc.) and displayed on a personal computer. The avalanche photodiode was aligned on the edge of a single backscattered fringe (the third fringe right of the centroid) at approximately $1/e^2$ of the essentially Gaussian-like intensity profile. A variation in signal was observed when the refractive index of the medium within the channel was altered, resulting in a positional shift of the backscattered fringe (Figure 2). Spatial movement of the backscattered fringe produced a change in the total light intensity striking the active area of the photodetector and a subsequent change in the output voltage of the detector.

PDMS Chip Preparation. The PDMS chips were prepared using previously reported microfluidic molding/imprinting procedures found in the scientific literature.[31-36] In summary, a positive relief mold of the desired microfluidic pattern is created using a photoresist and conventional photolithography on a Si or glass wafer. Then a degassed 10:1 mixture of Sylgard 184 elastomer and a curing agent (Dow Corning) is poured over the mold. After curing in the hot oven, the PDMS slab containing the microfluidic network is peeled from the mold and is sealed with another glass substrate, creating a fully functional microfluidic chip. It has been found in this laboratory that a 20 s oxidation in PDC 32G plasma cleaner (Harrick Scientific Co., Ossining, NY) of both the PDMS chip with the channels and a microscope slide was sufficient to create a permanent seal between both materials.

Surface Preparation. Reagent or better grade chemicals were chosen, and distilled, degassed Milli-Q water (18.4 MΩ/cm) was used in all experiments described in this paper. The following procedure was applied to irreversibly bind streptavidin to the PDMS channel walls. First, the channel was thoroughly rinsed with deionized water. Next, a 0.01% *p*-L-lysine (Sigma-Aldrich) solution was drawn through the

channel, and the channel was allowed to incubate for 10 min at room temperature (RT), followed by a thorough PBS rinse. A 12.5% solution of glutaraldehyde (Sigma-Aldrich) was then introduced into the channel, and the channel was allowed to sit for 45 min at RT and rinsed with PBS. After the PBS was withdrawn from the channel, it was filled with a 1 mg/mL solution of streptavidin (Sigma-Aldrich) and left undisturbed for 15 min at RT. Finally, a 40 mM solution of ethanolamine was introduced into the channel, and the channel was allowed to incubate for 15 min and flushed with PBS. As a result, the surface of the PDMS channel was coated with immobilized streptavidin for irreversible binding studies. For reversible protein-protein interaction studies a 2.5 mg/mL solution of biotinylated protein A (Sigma-Aldrich) was introduced into the immobilized streptavidin channel and allowed to bind to streptavidin for 5 min, forming an irreversible bond. As before, the unreacted protein A was flushed from the channel with a thorough PBS rinse.

Results and Discussion

BIRC for High-Sensitivity RI Detection in Rectangular PDMS Channels. Universal or label-free solute detection remains a challenge when microfluidic systems are employed.[4,36-38] Recent theory and experiments showed that OCIBD is a unique interferometer,[25] providing high sensitivity for label-free solute detection[26,28] for microfluidic systems. Yet, these observations were made using relatively expensive fused silica chips with channels containing curved surfaces due to the isotropic etching process.[39] In backscattering interferometry the channels or chip feature serves as the key optical element, and previous results indicated that the channel *curvature* played a role in the formation of the multipass configuration that leads to OCIBD's high sensitivity.[25,26] Ultimately it would be desirable to employ the less expensive and easier to prepare PDMS chips, yet they most often contain rectangular channels. Given previous observations with OCIBD, it was nonintuitive that a chip with rectangular channels would produce high-contrast interference fringes, or that the fringes would have high sensitivity to optical path length changes. Further, a preliminary optical ray trace modeling effort where the beam and the channel central axis are perpendicular gave discouraging results. Regardless, the simple optical configuration shown in Figure 1 was constructed. Figure 2 shows that much to our surprise a set of very high contrast interference fringes could be seen in the direct back-scatter direction. This surprising result was exciting considering the fringes are formed by simply illuminating a 90 × 40 μm fluid-filled rectangular channel molded in PDMS with an unfocused, inexpensive, low-power coherent light source. The contrast ratio of these fringes was amazingly similar to those produced from *semicircular* channels etched in fused silica, which has a relatively high reflectivity at 632.8 nm. It is noteworthy that the fringes are formed by an unmodified channel (no reflection coatings) in PDMS using established molding/imprinting procedures.[31-35] Figure 2 also shows that small alterations in the refractive index of the fluid within the channel result in a positional shift of the backscattered fringe pattern, indicating high finesse interference.

Evaluation of the BIRC system was then undertaken using a chip with a smaller channel (30 × 50 μm). Positional changes

(31) Duffy, D. C.; McDonald, J. C.; Schueller, O. J. A.; Whitesides, G. M. *Anal. Chem.* **1998**, *70*, 4974-4984.
(32) Wu, Z. Y.; Xanthopoulos, N.; Reymond, F.; Rossier, J. S.; Girault, H. H. *Electrophoresis* **2002**, *23*, 782-790.
(33) Anderson, J. R.; Chiu, D. T.; Jackman, R. J.; Cherniavskaya, O.; McDonald, J. C.; Wu, H. K.; Whitesides, S. H.; Whitesides, G. M. *Anal. Chem.* **2000**, *72*, 3158-3164.
(34) Martynova, L.; Locascio, L. E.; Gaitan, M.; Kramer, G. W.; Christensen, R. G.; MacCrehan, W. A. *Anal. Chem.* **1997**, *69*, 4783-4789.
(35) Tan, A. M.; Rodgers, K.; Murrihy, J. P.; O'Mathuna, C.; Glennon, J. D. *Lab Chip* **2001**, *1*, 7-9.
(36) Quake, S. R.; Scherer, A. *Science* **2000**, *290*, 1536-1540.
(37) Verpoorte, E.; Manz, A.; Ludi, H.; Bruno, A. E.; Maystre, F.; Krattiger, B.; Widmer, H. M.; Vanderschoot, B. H.; Derooij, N. F. *Sens. Actuators, B* **1992**, *6*, 66-70.
(38) Liang, Z. H.; Chiem, N.; Ocvirk, G.; Tang, T.; Fluri, K.; Harrison, D. J. *Anal. Chem.* **1996**, *68*, 1040-1046.
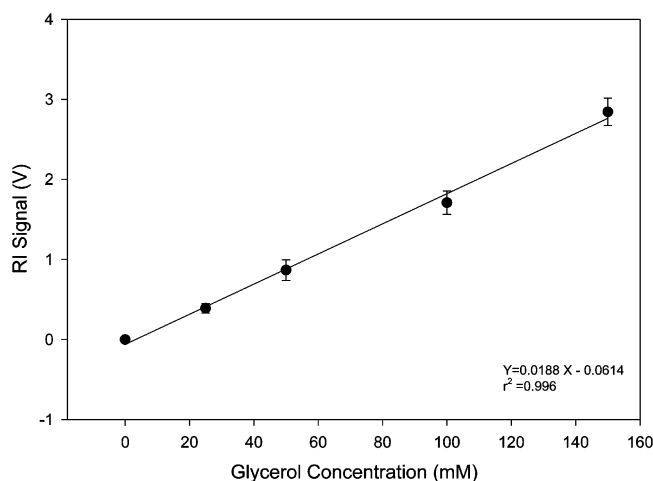(39) Kovacs, G. T. A. *Micromachined transducers sourcebook*; WCB McGraw-Hill: Boston, 1998.

Figure 3. Glycerol calibration curve for BIRC with rectangular channels molded in PDMS. Concentrations from 0 to 150 mM correspond to a 2×10^{-3} RI change. The 3σ detection limit was determined to be 8.32×10^{-6} RIU.

such as those observed in OCIBD can be monitored in BIRC with a phototransducer using a variety of previously published techniques;[25,26,29,30,40] here an apertured avalanche photodetector was chosen. First, the PDMS chip with microfluidic channels was securely mounted onto an insulated black anodized aluminum block, which provided passive thermal stabilization for the chip. Next, a set of fringes was obtained by illuminating a portion of the channel. The phototransducer was then positioned at the edge ($1/e^2$) of the third interference fringe. This alignment allows the portion of the fringe that has linear intensity changes with position to be sampled.[25,26,29] Sensitivity to RI changes was then evaluated using a series of solutions with varying concentrations of glycerol (0 and 150 mM). Spatial changes in the backscattered fringe pattern were interrogated as the glycerol solutions were introduced sequentially into the channel by a vacuum. Prior to collection of the output signal, each solution was allowed to pressure and temperature stabilize inside the channel. The resultant RI signal was recorded, and the channel was rinsed with deionized water. The calibration curve shown in Figure 3 represents a three-trial average that was linear ($r^2 = 0.996$) over a 2.5 decade change in concentration with a slope of 18.8 mV/mM. The 3σ detection limit was found to be 8.32×10^{-6} RIU for BIRC with rectangular channels molded in PDMS. This detection limit is slightly poorer, but compares well with that obtained with semicircular channels etched in fused silica.[25] Thus, minimal sensitivity loss was encountered due to a change in channel optical geometry from hemispherical or semicircular to rectangular and by employing these considerably less expensive and easier to prepare PDMS substrates.

An Irreversible Binding Study. Determination of binding constants and the detection of molecular interactions are central to understanding biological systems, important for monitoring priority pollutants, paramount in detecting biological or chemical weapons, and key in the efficient screening of potential drug candidates. The simplest and most widely practiced approach to perform such analyses often involves the use of the strong binding pair biotin and strepavidin.[11,16,41] Since this protein pair

often serves as a test system for a binding assay, it was employed to evaluate the suitability of BIRC for molecular binding determinations. The fluorescently labeled biotin also provides an alternative detection method for the verification of BIRC. First, streptavidin was immobilized on the inner surface of two 60 μm $\times$ 50 μm microfluidic channels (as described in the Experimental Section). Then blank fluorescent images of the PBS-filled channels were obtained (Figure 4A) using a Zeiss fluorescent microscope equipped with a Sensys Photometrics CCD camera and a fluorescein filter set (Chroma, Inc.). Next, the chip was mounted onto the holder and aligned. Once a baseline RI signal was established, PBS in the channel was replaced with a 1 mg/mL solution of FITC-labeled biotin (Sigma-Aldrich). The reaction between biotin and immobilized streptavidin was allowed to proceed for 1 min. Then unreacted biotin was completely washed from the channel and replaced with PBS. After a several minute pressure and temperature equilibration period the fringe position was quantified, allowing the change in RI signal (optical path length change) to be determined. This experiment was repeated twice using two different channels. The signal associated with biotin−streptavidin binding was calculated as the difference between the BIRC output before and after biotin interaction and with PBS in the channel. Once the interferometry signal for binding was obtained, fluorescent images were obtained with the microscope to confirm and quantify biotin−streptavidin binding. These images, taken with a 59 s exposure time, are shown in Figure 4B,C and clearly show FITC-labeled biotin is immobilized in the channel. The change in fluorescent signal between pre and post biotin binding was quantified by calculating the difference in the integrated fluorescence intensity gray scale values for each channel.

The binding of biotin to streptavidin was also verified using atomic force microscopy (AFM) in noncontact mode. A small piece of oxidized PDMS was cut from the chip and thoroughly washed. The streptavidin was immobilized on the surface following the same procedure as above and allowed to react with biotin. AFM surface profiles were taken after each preparation step and are displayed in Figure 5: bare washed PDMS, PDMS with immobilized streptavidin, and PDMS with immobilized streptavidin−biotin complex. As can be seen from these images, streptavidin was bound to the PDMS surface and did react with FITC-labeled biotin using the same chemistry as in the BIRC experiments.

Figure 6 presents a bar graph depicting the BIRC signal obtained from the microfluidic channels before and after reaction with biotin. Each bar corresponds to the unfiltered signal collected for 30 s, and the error bars represent the standard deviation in the signal during that time period. Plotted in the figure inset is the change in signal from channel 1 to channel 2 for BIRC and the fluorescence detection schemes. When the results of the two trials were compared (channel 1 to channel 2), more binding of biotin to streptavidin occurred in the first channel than the second channel, which was indicated by both a stronger fluorescent signal and a larger RI signal. In both the interferometric and fluorescence analyses, the change in signal decreased by approximately 50% from channel 1 to channel 2 (51% for RI and 56% for fluorescence). This difference is attributed to less streptavidin immobilized onto the surface of

(40) Markov, D.; Begari, D.; Bornhop, D. J. *Anal. Chem.* **2002**, *74*, 5438−5441.

(41) Brooks, S. A.; Dontha, N.; Davis, C. B.; Stuart, J. K.; O'Neill, G.; Kuhr, W. G. *Anal. Chem.* **2000**, *72*, 3253−3259.
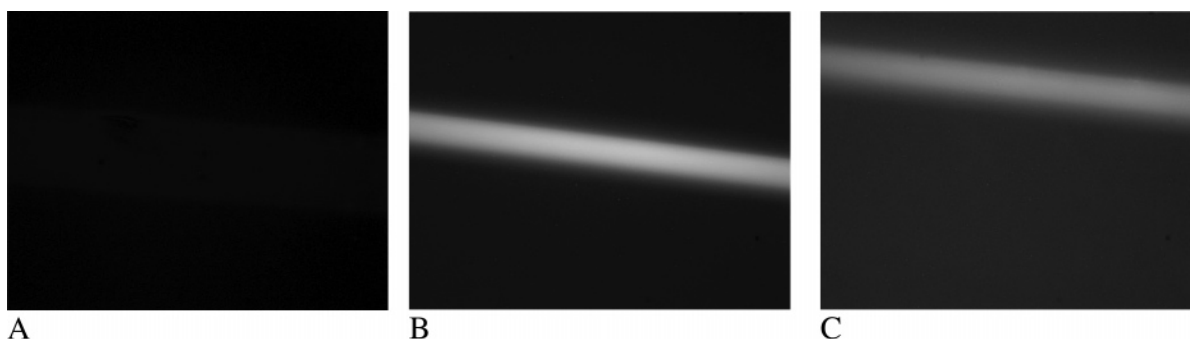
Figure 4. Fluorescent pictures of PDMS channels (exposure 59 s): (A) channel 1, surface-bound streptavidin (blank); (B) channel 1, surface-bound streptavidin reacted with FITC-labeled biotin; (C) repeated experiment in channel 2, surface-bound streptavidin reacted with FITC-labeled biotin. The channel 2 fluorescent blank showed no fluorescence (not shown).
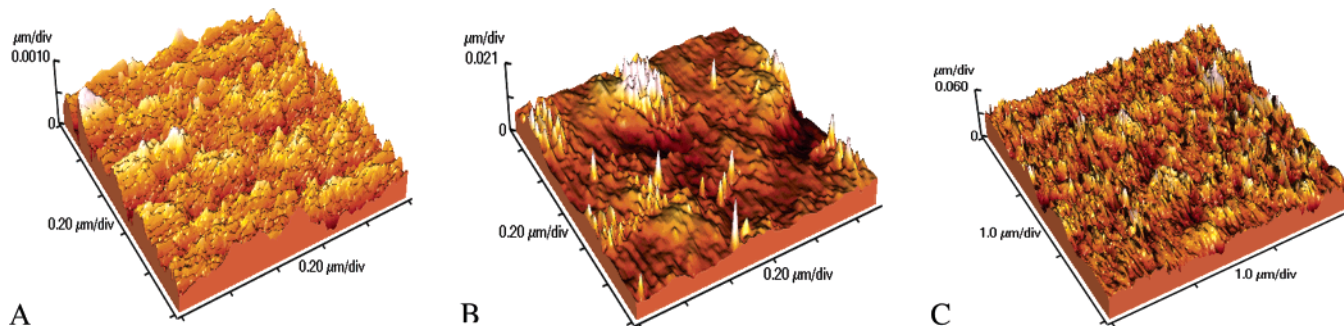

Figure 5. Atomic force microscopy images of (A) bare PDMS, (B) PDMS with immobilized streptavidin, and (C) biotin bound to immobilized streptavidin.
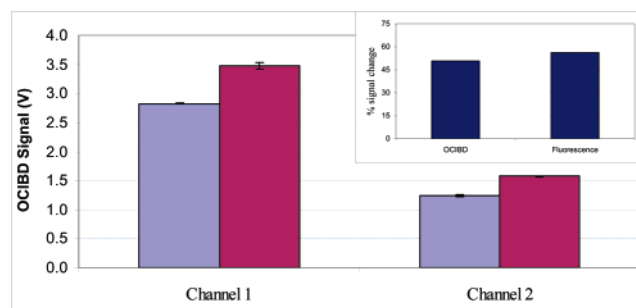

Figure 6. BIRC signal generated by two identical channels and as a result of interaction between surface-bound streptavidin and FITC-labeled biotin: light purple, surface-bound streptavidin in PBS buffer; burgundy, surface-bound sterptavidin–biotin complex in PBS buffer. The inset shows the percent signal change between channel 1 and 2 determinations, due to the binding event, allowing comparison of the response for BIRC and fluorescence.

the second channel. The results are consistent between the BIRC and the complementary imaging method of fluorescence microscopy.

Assuming that the total noise present in the BIRC output for streptavidin–biotin binding is a zero mean Gaussian process, its root-mean-square value can be calculated to be 0.0564 V. This value corresponds to a measure of the noise in the system. Thus, an RI signal of 0.65 V yields a signal-to-noise ratio (S/N) of 11.5 (21.2 dB) for the biotin–streptavidin experiment performed in channel 1. The mass detection limit for biotin bound to streptavidin can be estimated by assuming (a) the response of BIRC is linear and (b) in the worst-case scenario, all biotin present in the 225 pL probe volume reacted with immobilized streptavidin. Under this scenario a ratiometric analysis can be used to estimate the minimum quantity (mass) of biotin that can be detected. At 2σ this value corresponds to 19×10^{-12} g or 47 fmol of biotin.

A Reversible Binding Study. Having used BIRC with PDMS chips successfully for the analysis of biotin–streptavidin irreversible binding, the more challenging investigation of reversible protein–protein interactions was undertaken. Similar to investigations undertaken by Sailor et al. with porous Si,[7,11] the reversible binding of protein A and human IgG (F_c fragment) was monitored with BIRC. Biotinylated protein A was immobilized onto the PDMS channel surface using the procedure detailed in the Experimental Section, the channel was filled with PBS, and the system was aligned to produce high-contrast fringes. Then, a 2.5 mg/mL human IgG F_c (Calbiochem Corp.) solution (in PBS) was introduced into the channel, allowing the IgG to bind to protein A for 5 min. Next, the channel was rinsed with PBS to remove unreacted IgG, and the interference signal was quantified. Reversal of the IgG–protein A binding (removal of the bound IgG from protein A) was then accomplished by incubation of the microfluidic channel with 0.1 M acetic acid for 5 min. The chip was then filled with PBS and the interferometry signal quantified. Figure 7 shows the OCIBD signal corresponds to a level similar to that before binding and removal of IgG. This procedure was iterated several times, allowing the determination of reversible molecular interactions. As a control a noncomplimentary fragment, F_{ab}, was tested using an identical procedure. No signal was observed for the control, also illustrating that there is minimal nonspecific binding and showing the potential of the technique.

The summary of the results from the reversible binding assay is shown in Figure 7. Depicted are the observed changes in the BIRC signal for a typical IgG F_c reversible binding determination. Good temporal stability of the detector with no electronic filtering during the measurement cycle was observed. As can be seen from the graphs in Figure 7A, the binding of human IgG F_c (2.5 mg/mL) to protein A repeatedly produced (three-trial average) a change in signal equal to 0.289 ± 0.0166 V,
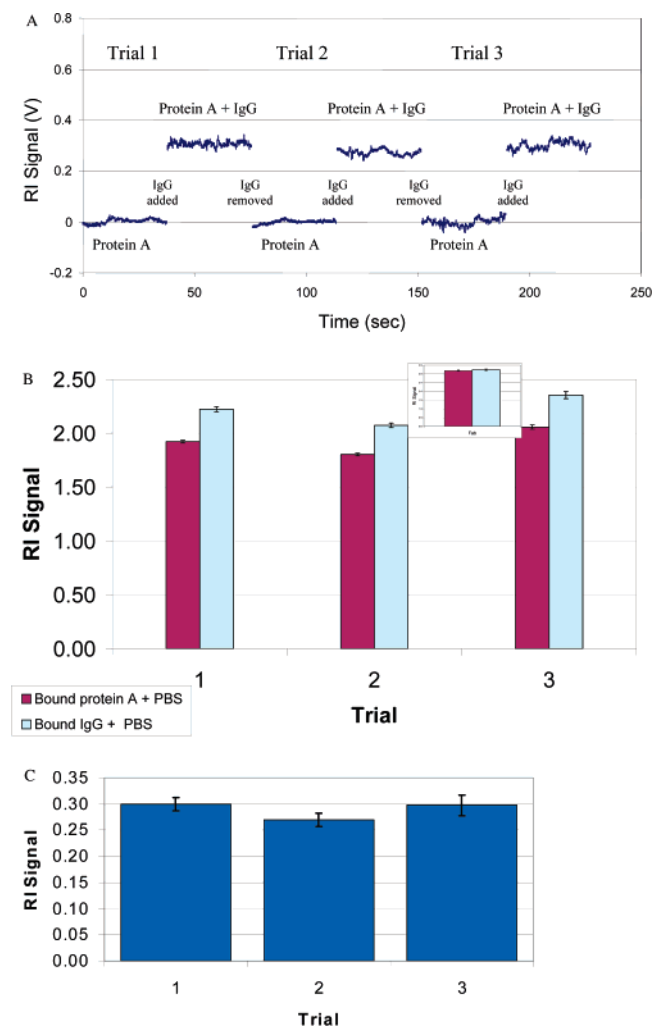
Figure 7. (A) A typical temporal response of BIRC for the relative signal change due to the IgG F_c binding event. (B) BIRC signal produced by sequential binding and unbinding of human IgG F_c to the surface-immobilized protein A. The inset depicts no change in signal for a noncomplementary fragment F_{ab}. (C) Average BIRC signal produced by IgG F_c binding to protein A.

leading to a signal-to-noise ratio of 17.41 (24.8 dB). Even though the overall light intensity changed during the third run due to the instability of the semiconductor laser, resulting in an increased baseline signal and larger error bars (Figure 7B, trial 3), the relative change in the signal due to the presence or absence of IgG was consistent and reproducible for the repetitive binding events (Figure 7A,C). This observation shows the robust nature and inherent high S/N possible with BIRC. Assuming 100% solute–substrate interaction, meaning that all of the human IgG F_c present in the probe volume was bound to protein A, a conservative estimate of the 3σ detection limit is 2×10^{-15} mol of IgG bound to protein A. This value corresponds to a mass detection limit of 10 pg for IgG. The concentration detection limit for this label-free protein–protein binding assay performed in a PDMS chip with BIRC was found to be 0.4

mg/mL. The control, a 2.5 mg/mL solution of IgG F_{ab} (Calbiochem Corp.) in PBS, gave no quantifiable change in signal (0.048 ± 0.043 V) when it was studied as described above. These observations further confirm that OCIBD performed with microfluidic channels molded in PDMS can be used to monitor label-free protein–protein interactions and that the optical path length changes induced by molecular interactions translate into a sensitive measurement method.

Conclusions

We have shown for the first time that label-free reversible molecular interaction determinations can be successfully performed within a microfluidic network molded in inexpensive plastic. Detection was performed using a unique, simple, and highly sensitive method based on backscattering interferometry. The rectangular channels serve both as the microfluidic network and as the optical element of the picoliter volume (225 pL) interferometer. In addition to facilitating the determination of label-free protein–protein interactions, the unique detection technology was shown to be useful for monitoring bulk refractive index changes as well. Both reversible and irreversible protein–protein interactions were studied in a noninvasive, fashion providing femtomole detection limits (2×10^{-15} and 47×10^{-15} mol for human IgG F_c and biotin, respectively). These detection limits were obtained in the absence of electronic filtering while using only passive thermal stabilization.

Given the high sensitivity and large dynamic range of BIRC with respect to solute concentration, we predict it will be possible to noninvasively quantify binding affinities and binding constants in small volumes. Additionally, BIRC can potentially be used to monitor protein/ligand binding events as they progress within microfluidic channels. Incorporation of a reference channel aids in this effort, allowing for a more quantitative analysis through the compensation of the nonsignal (binding event) RI changes. Currently, we are in the process of implementing such a system.

In general, BIRC represents a unique approach to performing interferometry that utilizes a very simple and inexpensive optical train, with economical disposable chips. The system appears to be scalable without loss of sensitivity and is amenable to integration for high-throughput determinations. BIRC has been shown to facilitate label-free molecular interaction determinations with femtomoles of solute and has high potential for quantification of binding affinities.